Atmospheric Environment 44 (2010) 2147–2156

Contents lists available at ScienceDirect

Atmospheric Environment

journal homepage: www.elsevier.com/locate/atmosenv

Physical characterization of the fine particle emissions from commercial aircraft engines during the Aircraft Particle Emissions eXperiment (APEX) 1–3

John S. Kinsey [a,*], Yuanji Dong [b], D. Craig Williams [b], Russell Logan [b]

[a] U.S. Environmental Protection Agency, Office of Research and Development, National Risk Management Research Laboratory, MD E343-02, Research Triangle Park, NC 27711, USA
[b] ARCADIS U.S., Inc., 4915-F Prospectus Drive, Durham, NC 27713, USA

ARTICLE INFO

Article history:
Received 14 August 2009
Received in revised form
4 February 2010
Accepted 8 February 2010

Keywords:
Particulate matter
Emissions
Gas turbine engines
Aircraft
Ground measurements

ABSTRACT

The fine particulate matter (PM) emissions from nine commercial aircraft engine models were determined by plume sampling during the three field campaigns of the Aircraft Particle Emissions Experiment (APEX). Ground-based measurements were made primarily at 30 m behind the engine for PM mass and number concentration, particle size distribution, and total volatile matter using both time-integrated and continuous sampling techniques. The experimental results showed a PM mass emission index (EI) ranging from 10 to 550 mg kg^{-1} fuel depending on engine type and test parameters as well as a characteristic U-shaped curve of the mass EI with increasing fuel flow for the turbofan engines tested. Also, the Teflon filter sampling indicated that ~40–80% of the total PM mass on a test-average basis was comprised of volatile matter (sulfur and organics) for most engines sampled. The number EIs, on the other hand, varied from ~10^{15} to 10^{17} particles kg^{-1} fuel with the turbofan engines exhibiting a logarithmic decay with increasing fuel flow. Finally, the particle size distributions of the emissions exhibited a single primary mode that were lognormally distributed with a minor accumulation mode also observed at higher powers for all engines tested. The geometric (number) mean particle diameter ranged from 9.4 to 37 nm and the geometric standard deviation ranged from 1.3 to 2.3 depending on engine type, fuel flow, and test conditions.

Published by Elsevier Ltd.

1. Introduction

The fine particulate matter (PM) emissions from aircraft operations at large airports located in areas of the U. S. designated as non-attainment for the National Ambient Air Quality Standard (NAAQS) for PM (particles ≤2.5 μm in aerodynamic diameter) are of major environmental concern (Waitz et al., 2004). Aircraft PM at cruise conditions is also important in the formation of contrails and contrail-induced cirrus clouds at high altitude with their projected impact on the global climate (Penner et al., 1999; Sausen et al., 2005; Wuebbles et al., 2007). In general, the majority of the available PM emissions data for commercial aircraft engines is limited and does not completely characterize volatile components resulting from atmospheric cooling and dilution (Wayson et al., 2009; Webb et al., 2008). There is, therefore, the need for a comprehensive PM emissions database for aircraft turbine engines which include mass-based emission indices and chemical speciation data and which also relate the PM emissions to key engine operating parameters and fuel characteristics.

To address the need for improved aircraft PM emissions data, the Aircraft Particle Emissions eXperiment (APEX) was organized in 2003. The APEX program is a major collaborative effort between the National Aeronautics and Space Administration (NASA) and a number of other research organizations including the U.S. Environmental Protection Agency's (EPA's) National Risk Management Research Laboratory (NRMRL) in Research Triangle Park, North Carolina (Wey et al., 2007; Lobo et al., 2007a). The EPA objectives of the three APEX sampling campaigns (APEX-1, -2, and -3) were to update and improve emission factors (indices) and chemical source profiles for aircraft-generated fine PM and, if possible, assess the effect of engine operating conditions (e.g., cold vs. warm) and fuel properties (e.g., sulfur content) on PM formation.

This paper provides the results of ground-based emission measurements conducted by EPA in the engine exhaust plume during APEX-1, -2 and -3. This research used the EPA's Diesel Emissions Aerosol Laboratory (DEAL) as the sampling platform and resulted in the first EPA-generated emission indices for commercial aircraft engines since the late 1970s. The following sections provide a brief description of the APEX research as related to the physical characteristics of the fine PM emissions from nine engine models

* Corresponding author. Tel.: +1 9195414121; fax: +1 9195410359.
E-mail addresses: kinsey.john@epa.gov (J.S. Kinsey), yuanji.dong@arcadis-us.com (Y. Dong), williams.craig@epa.gov (D.C. Williams), logan.russ@epa.gov (R. Logan).

1352-2310/$ – see front matter Published by Elsevier Ltd.
doi:10.1016/j.atmosenv.2010.02.010

along with an assessment of operating temperature and fuel effects. More detailed data, including the gas- and particle-phase chemical speciation results, can be found in Kinsey (2009).

2. Plume sampling system

2.1. Sample probe and lines

The DEAL's sample extraction system was used to collect an air sample at the centerline of the engine exhaust plume at a single point downstream from the engine exit plane. The system was configured as a tapered, beveled nozzle connected to a 5-cm outside diameter (OD) polished stainless steel sampling line that ran from the plume centerline to the inlet of the DEAL's instrumented sampling tunnel. Thoroughly cleaned stainless steel tubing and fittings were used for the entire system. The sampling probe (see Supporting information) was attached to a rigid stand anchored to the tarmac.

The exact length and configuration of the EPA sampling line running from the probe to the DEAL depended on the engine type and sampling campaign. In APEX-1 and -2 sampling was conducted only at 30 m behind the engine, whereas in APEX-3, measurement probes were also located at 15 and 43 m to accommodate the wide variety of engines tested. For the APEX-3 sampling, pneumatic valves were used to sequentially switch back and forth between probes at two distances behind the engine (i.e., 15- or 30-m; 30- or 43-m) to evaluate plume aging effects. Since sampling was always conducted at the 30-m position, only these data are presented in this paper except where noted.

Particle losses inside the long sample extraction system between the probe inlet and the sampling tunnel were a major concern. Therefore, in a separate experiment to characterize particle losses (Kinsey, 2009), the exhaust from the DEAL's Kenworth diesel tractor diluted with ambient air was introduced into the inlet of the APEX sample probe. Particle size distributions and number concentrations were then measured and recorded using a TSI Model 3090 Engine Exhaust Particle Sizer (EEPS) at two locations: (1) at the probe inlet; and (2) inside the DEAL sampling tunnel. The sampling system configuration for each APEX sampling campaign was setup exactly the same as was used in the field. Using the EEPS data collected, a series of particle penetration curves was generated for the three APEX sampling systems as described by Kinsey (2009).

2.2. DEAL measurement system

The DEAL uses two centrifugal blowers, each controlled by a variable frequency drive and mass flow meter, to continuously extract 1.1 (actual) m^3 min^{-1} of sample gas from the plume (Kinsey et al., 2006). After extraction, the plume sample flows through a 5-cm diameter stainless steel sampling tube into a PM-2.5 "cut point" (i.e., particle diameter representing a 50% collection efficiency for equivalent unit density spheres $\leq$2.5 μm in aerodynamic diameter) virtual impactor, and then into an 8.8-m long, 15-cm inside diameter (ID) stainless steel sampling tunnel. A series of "button hook" stack sampling nozzles, increasing in height along the length of the tunnel to minimize aerodynamic interference, are used to extract samples from the tunnel. The sample flow captured by each nozzle exits the sampling tunnel through custom designed four-way flow splitters that direct the flow from the tunnel to the various instruments. Either grounded stainless steel or conductive silicone rubber lines connect the instruments to the appropriate sample splitter. A similar sampling system was also used for characterization of the ambient background as described by Kinsey (2009).

Fig. 1 is representative of the DEAL instrumentation package used for speciated testing during the APEX campaigns for both the engine exhaust and the ambient background (Kinsey, 2009). In this context, "speciated" refers to those tests designated for the determination of gas- and particle-phase chemical characteristics by time-integrated sampling.

During the three APEX campaigns, both continuous monitoring and time-integrated sampling (Fig. 1) was conducted for both particle- and gas-phase air pollutants. Continuous monitoring was conducted for: PM mass and number concentration, particle size distribution, black carbon, particle surface polycyclic aromatic hydrocarbons, carbon dioxide, carbon monoxide (APEX-1 only), total volatile organic compounds (APEX-1 only), plume temperature and velocity (APEX-2 only), and ambient temperature, relative humidity, and wind speed/direction. Time-integrated sampling was also performed for PM mass concentration (Teflon filter), total volatile PM (i.e., Teflon filter sampling downstream of a thermal denuder), elemental/organic carbon, speciated semi-volatile organic compounds, speciated water-soluble ions, elemental composition, gas-phase non-methane volatile organic compounds, and gas-phase carbonyls. A complete list of all parameters measured along with the sampling location, type of sample, and specific instruments employed in the three APEX campaigns is provided in Table S-1 of the Supporting information (Kinsey, 2009).

The DEAL is also equipped with a computerized data acquisition system (DAS) to continuously record the experimental data being collected from the various instruments and samplers. The DAS consists of a multi-computer network containing up to eight CPUs plus a computerized operator's station. The network is time synchronized using the master computer clock which is set daily to an atomic clock traceable to the National Institute of Standards and Technology (NIST).

3. Measurement protocols

3.1. Pre-test procedures

Prior to each sampling campaign, initial cleaning of the sampling tunnels and lines was conducted by power washing all internal surfaces using a dilute solution of laboratory detergent in deionized (DI) water, followed by a DI water rinse. After power washing, the equipment was allowed to air dry and capped at both ends for transport to the field.

Following the setup of each sampling system in the field, and prior to any sample collection, positive pressure leak checks were performed on both the sampling line and sampling tunnel inside the DEAL. This was done by pressurizing each system to about 260 mm mercury (Hg) with compressed air from a cylinder. If the pressure dropped, the system was re-pressurized and all the flange joints and other fittings were checked for leaks using a soap and water mixture while pressure was maintained on the system. The system was deemed to be leak free when the cylinder pressure could be adequately maintained for a period of about 5 min.

All sampling media (see Kinsey et al., 2009 for details) were prepared in NRMRL's Fine Particle Characterization Laboratory (FPCL) before leaving for the field and stored inside a laboratory freezer maintained at −50 °C. During transport and in the field laboratory, all sampling media were stored in a small portable freezer operated at a nominal temperature of approximately −20 °C. The SUMMA canisters were stored under ambient conditions before and after sampling.

3.2. Field sampling procedures

A consistent and rigorous routine was followed to ensure proper operation of all the instruments during each sampling campaign. Miscellaneous operating procedures (MOP) and quality control

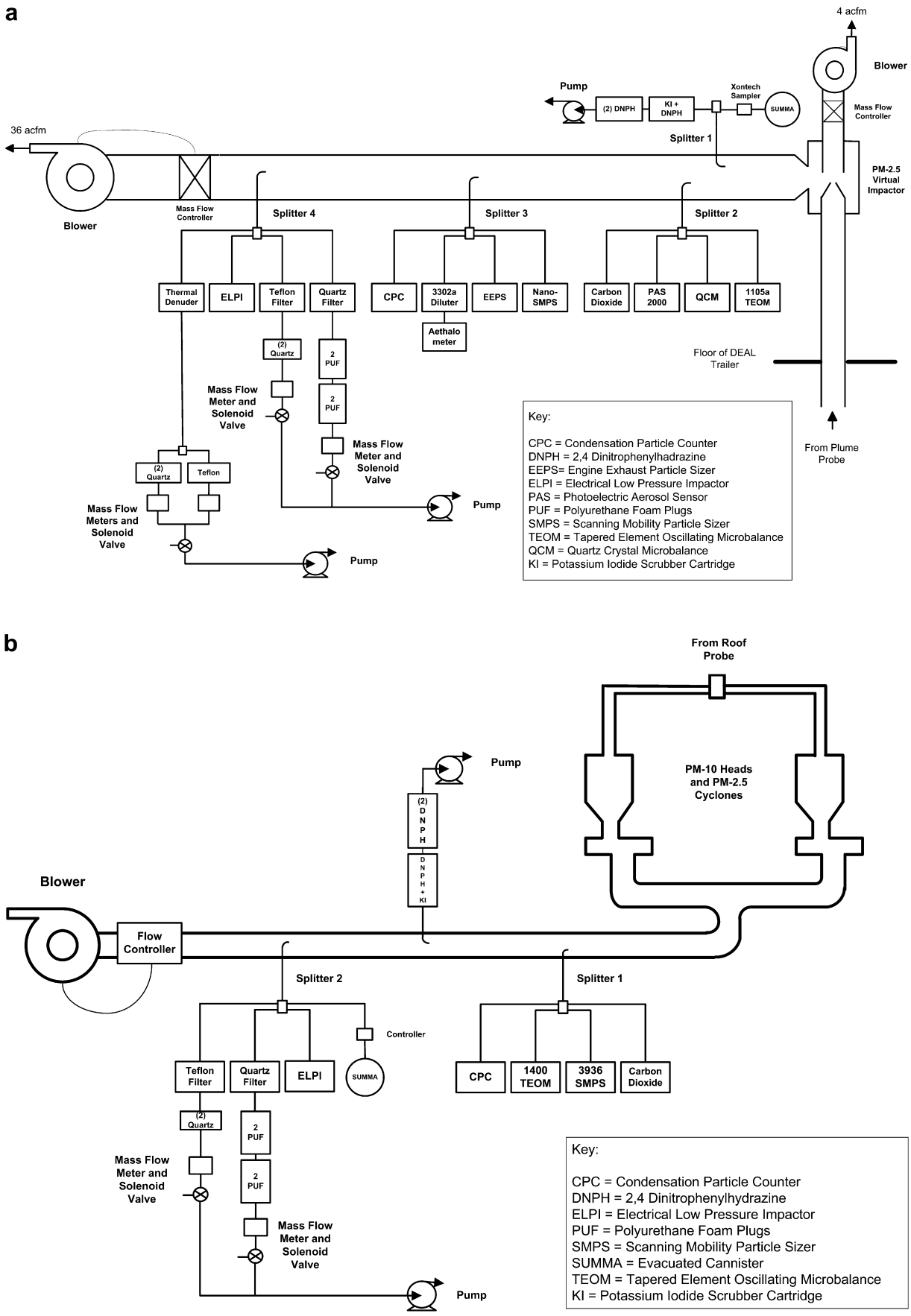

Fig. 1. Representative equipment configuration for speciated testing of: (a) engine exhaust plume; and (b) ambient background. See text.

(QC) checks were developed for each instrument as outlined in the approved quality assurance project plan (QAPP). Sample substrates (filters, canisters, adsorbent cartridges) were prepared in advance and the sample ID recorded on special data forms at the time of loading into each sampler. All continuous gas analyzers were also calibrated prior to being deployed to the field and checked twice daily thereafter. Finally, a blank test was conducted at the conclusion of each campaign with all instrumentation operating as in prior speciated tests except that only high efficiency particulate air (HEPA) filtered ambient air was sampled.

3.3. Post-test Teflon filter analyses

After returning from the field, all sampling media except the SUMMA canisters were stored continuously at −20 °C or below. The PM gravimetric analyses were performed by weighing the individual Teflon filters before and after sampling on a Sartorius microbalance with a detection limit of ±3 μg. The filter weighing was done in accordance with the procedure described by Title 40 of the U. S. Code of Federal Regulations (40CFR), Part 53 for ambient sampling (Kinsey, 2009). The method requires that the filter samples be conditioned before weighing, by exposure for a minimum of 24 h to an environmental chamber that is maintained at 20–23 °C and a relative humidity of 30–40%. To eliminate possible electrical charge from accumulating on the surface, both sides of each Teflon filter were exposed to polonium strips for at least 20 s before placing on the balance. The weight change in the same filter after sampling was then used for PM mass emission calculation.

3.4. Data analysis procedures

The measurements made by the TSI Model 3936 Scanning Mobility Particle Sizer (SMPS) equipped with a Model 3080 Electrostatic Classifier and Model 3085 Nano Differential Mobility Analyzer (nano-SMPS), TSI EEPS, and Dekati Electrical Low Pressure Impactor (ELPI) provided the particle number concentrations under various test conditions. Although the ELPI was not useful in this study for the determination of particle size distribution due to the relatively large cut-off size of its lowest channel, the use of a filter stage enabled the instrument to measure the total particle number concentration. Note that the nano-SMPS and EEPS were only operated in the plume sampling system of the DEAL. Therefore, for the nano-SMPS, the ambient background was determined before and after each test and averaged to correct the data. The EEPS data were not background corrected since it was determined that the background had a negligible effect. Note also that the EEPS was not available during the APEX-1 campaign and the ELPI was not operated during some APEX-1 tests (NASA 1 and NASA 5) and APEX-3 tests (T2, T5, T8 and T10) due to the recovery of the impactor substrates for possible organic speciation. Except where noted, only data corrected for particle losses in the sampling line are presented.

The PM mass emissions were calculated by converting the PM number concentration data measured by the nano-SMPS and EEPS into the PM mass concentrations assuming unit density and spherical morphology. It should also be recalled that the nano-SMPS and EEPS were only used in the plume sampling system and thus were background corrected as described previously.

The mass emissions for different jet engines were also determined on a test-average basis from the Teflon filter sampling both with and without a Dekati Model EKA-111 thermal denuder (set to a temperature of 250 °C) to determine total volatiles. The PM mass emission index (EI_m) obtained from a filter sample was an average value over all engine power conditions for an entire test including start-up, shut down and transitions. The percent volatile matter in the PM collected by a Teflon filter for each test was calculated by dividing the difference in the PM mass concentration before and after the thermal denuder by that determined from the filter without the denuder. The volatile PM measured by this technique was produced by the gas-to-particle conversion of sulfur and organic gases as the plume cools and dilutes in the atmosphere (Kinsey, 2009; Wayson et al., 2009).

Finally, the particle size distribution (PSD) of the emissions from the various engines tested during the three APEX campaigns were determined by the nano-SMPS and EEPS instruments. Note, however, that the nano-SMPS had a response time of approximately 2.5 min making it difficult to obtain data under the highest engine power settings. Therefore, no PSDs for the 100% power setting (take-off) are reported for the nano-SMPS, and limited data are reported for the 85% power setting (climb).

The differential number PSD, dN/dlogDp, at a specified power setting was obtained by averaging the particle numbers recorded under the same engine operating condition from the same instrument particle size bins and then plotting them against the particle size. The average dN/dlogDp data for each power setting was then smoothed over the entire size range using the "supsmooth" function provided by the MathCad 2001 Professional software package. The geometric number mean diameter (GMD) and geometric standard deviation (GSD) were then calculated over the entire particle size range as a function of fuel flow rate as described by Kinsey (2009).

Emission indices were calculated from the experimental data in terms of mass (or number) of pollutant per 10^3 mass units of fuel burned (e.g., mg kg^{-1} fuel) using a carbon balance involving the percent carbon in the fuel determined by fuel analysis and the concentration of carbon dioxide measured in the sample stream (note that the concentration of CO and total hydrocarbons are generally insignificant compared to CO_2). The experimental data were always presented in terms of the engine fuel flow recorded during each test but sometimes are shown relative to nominal percent rated thrust for ease of comparison between different engine types.

4. Test engines, fuels, and operating schedule

There were a total of 24 tests conducted by EPA during the three APEX campaigns. A CFM International CFM56-2C1 engine mounted on a DC-8 airframe was used throughout the nine APEX-1 tests to investigate the effects of fuel composition on emissions at various power settings. Three types of fuel were used: a base fuel (JP-8 or Jet-A1), a high-sulfur fuel (JP-8 doped with approximately four times the sulfur content of the base fuel), and a higher-aromatic JP-8.

During APEX-2 and -3, each engine was run with the available Jet-A fleet fuel it would use during normal commercial operations. The same engine family used during APEX-1, the CFM56 (in use on B737 airframes), was also included in all four APEX-2 tests and two of the eleven APEX-3 tests. These tests provided further characterization of the fine particulate emissions from these widely-used jet engines.

Five additional turbine engines of various sizes were also studied in APEX-3. These included a General Electric CJ610-8ATJ turbojet (in use on a Lear Model 25), Rolls Royce AE3007A1E and AE3007A1/1 mixed turbofans (in use on the Embraer ERJ145), a Pratt and Whitney PW4158 turbofan (in use on the Airbus A300), and a Rolls Royce RB211-535E4-B mixed turbofan (in use on the B757). Table 1 summarizes the specific engines tested and composition of the fuels used during the APEX campaigns along with the applicable test numbers and average ambient conditions occurring during each test. Certification values for ICAO-regulated smoke number are also provided in Table S-2 of the Supporting information for each engine tested.

Table 1
Test engines and fuels for APEX 1–3.

Campaign		Airframe	Engine model[a]	Bypass ratio[b]	Engine pressure ratio[b]	Rated thrust (kN)[b]	Fuel type	Fuel sulfur (ppm)[c]	Fuel aromatics (vol%)[c]	Average ambient temperature (°C)	Average ambient relative humidity (%)
APEX	Test no.										
1	EPA 1	DC-8	CFM56-2C1	6.0	23.5	97.86	Base	409	17.5	29	9
	EPA 2									20	19
	NASA 1									32	6
	NASA 1a									17	24
	EPA 3						High Sulfur	1639	17.3	25	6
	NASA 2									33	6
	NASA 3									25	11
	NASA 4						High Aromatic	553	21.8	30	12
	NASA 5									20	15
2	T1	B737-700	CFM56-7B24	5.2	25.8	107.7	Fleet Fuel	132	19.7	13	92
	T4							412	20.3	14	83
	T2	B737-300	CFM56-3B1	5.1	22.4	89.41	Fleet Fuel	206	20.4	14	82
	T3		CFM56-3B2	5.1	24.1	98.30		352	22.7	14	83
3	T1	B737-300	CFM56-3B1	5.1	22.4	89.41	Fleet Fuel	700	17.4	8	87
	T11							400	16.8	13	49
	T2 & T5	Lear 25	CJ610-8ATJ	N/A	~7	13.12	Fleet Fuel	0[d]	14.5	18	46
	T3 & T4	ERJ145	AE3007A1E[e]	4.8	17.8	33.7	Fleet Fuel	300	19.9	13	47
	T10		AE3007A1/1[e]	4.8	17.9	34.74		200	18.6	9	67
	T6 & T7	A300	P&W 4158	4.6	30.7	258.0	Fleet Fuel	600	16.5	19	69
	T8	B757	RB211-535E4-B[e]	4.1	27.9	191.7	Fleet Fuel	300	19.4	17	78
	T9							300	19.1	10	68

[a] All engines are turbofan except the CJ610-8ATJ which is a turbojet engine.
[b] Civil Turbojet/Turbofan Specifications (http://www.jet-engine.net/civtfspec.html) or International Civil Aviation Organization (ICAO) Emissions Databank Issue 15C.
[c] All fuel analyses performed by outside organizations. No information available on precision/accuracy of the analytical results.
[d] Questionable value as reported by NASA. Actual sulfur content should be similar to other APEX-3 tests.
[e] Internally mixed engines where core and bypass flow are combined prior to discharge to the atmosphere.

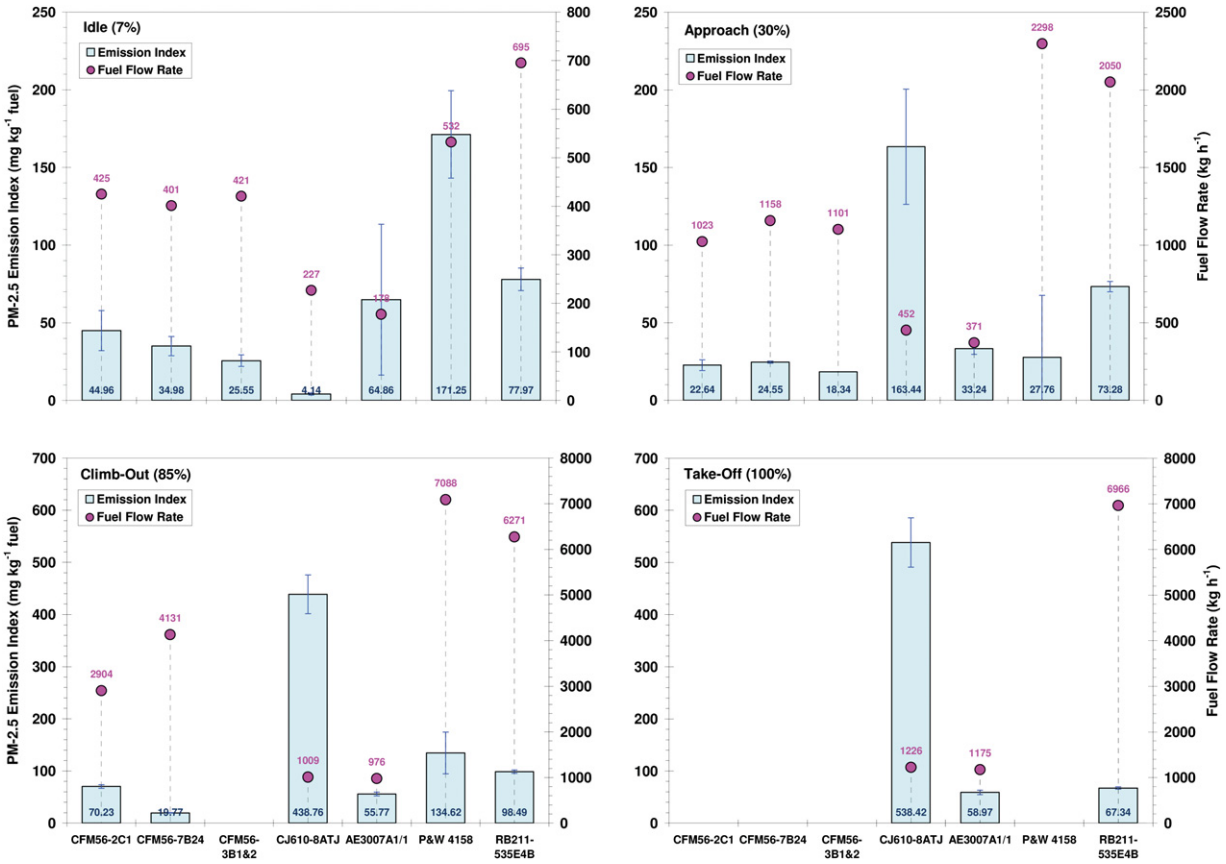

Fig. 2. Comparison of the PM EI_m for seven engine models operated at the four ICAO-specified engine thrust levels as determined by the nano-SMPS. Also note the average fuel flow shown as a dot in these graphs. P&W 4158 data for climb-out are at 80% thrust.

One item worthy of note is the wide variation in sulfur content of the standard fleet fuels used during the three tests on the same engine model, the CFM56-3B1. During APEX-2, Test 2, the fuel sulfur content was 206 ppm, whereas for the two APEX-3 tests, the sulfur content was 700 ppm (Test 1) and 400 ppm (Test 11).

In general, the test engines were operated at a series of steady-state power conditions which were set for the environmental conditions using the expertise of the on-site engine company representative. During APEX-1, two engine test matrices were used. The "EPA" test matrix followed the landing and take-off (LTO) cycle defined by the ICAO to simulate aircraft emissions at an airport and is heavily weighted to the idle power condition with its associated higher proportion of unburned organics in the exhaust stream. This matrix consisted of approximately four repetitions of the following power settings: 26 min at idle (7% rated thrust), 0.7 min at take-off (100%), 2.2 min at climb (85%), and 4 min at approach (30%). The "NASA" test matrix was designed to investigate the effects of engine operating parameters on particle emissions and included 11 power settings. Except for the 100% thrust level, where run-time was limited to 1.5 min, approximately 10 min were provided at each power setting to allow for samples to be adequately analyzed.

For APEX-2 and -3, the engines were operated in cycles encompassing a series of steady-state power settings to investigate their effects on particle emissions. The power levels include those used during engine certification, simulated cruise, engine start/stop, and transitions between throttle settings. During these tests, the thrust was changed in a stepwise fashion from the lowest thrust level to highest under the "cold" engine condition, and then decreased in a similar fashion under the "warm" engine condition. The specific power conditions and fuel flow varied by campaign and engine type and are detailed in Table S-3 of the Supporting information. Also note that no two tests were exactly alike with respect to engine operation during any of the APEX campaigns. This lack of consistency influenced the results of the time-integrated sampling discussed below.

5. Experimental results

The mass and number emission indices and their associated particle size distributions and volatile content were generated from data collected using either a nano-SMPS, EEPS, ELPI, and/or a 47-mm Teflon filter sampler both with and without an upstream thermal denuder in the plume sampling tunnel. A summary of the specific tests conducted during the three APEX campaigns is also provided in Table S-3 of the Supporting information (Kinsey, 2009).

5.1. PM mass emission indices by continuous methods

The PM mass emission index (EI_m) converted from the nano-SMPS data varied from 10 to 550 mg kg^{-1} and was found to be correlated to the rated engine thrust as a function of fuel flow rate. The relationship of fuel flow to EI_m was found to be generally similar for all turbofan engines tested (Kinsey, 2009). A characteristic U-shaped curve of EI_m vs. fuel flow was observed where the emissions are highest at idle, decrease to a minimum at mid-range power, and then increase again at higher engine power (see Supporting information). This was not the case for the turbojet engine tested in APEX-3 (CJ610-8ATJ), however, where the EI_m increases linearly with increasing fuel flow.

The magnitude of the mass EI was also found to vary by engine type. These variations are illustrated in Fig. 2 which compares the nano-SMPS data for seven engine models as operated at the four ICAO-specified LTO engine thrust levels. Note that there are no nano-SMPS data available for the CFM56-3B1 and -3B2 for 85 and 100% power. In addition, the P&W 4158 was not operated at 100% thrust. Therefore, no results are provided for these experimental conditions in Fig. 2.

As can be seen from Fig. 2, the smallest engine tested (CJ610-8ATJ turbojet) had the lowest EI_m at 7% idle power, whereas the largest engine evaluated (P&W 4158) exhibited the highest. The CJ610-8ATJ turbojet also displayed the largest EI_m for 100% take-off, 85% climb-out, and 30% approach, which is probably a function of its older combustor design. In addition, relatively good agreement in EI_m was shown for the three CFM56 variants tested, with the exception of climb-out.

Both engine operating temperature and fuel composition were also found to influence PM mass emissions. With respect to engine operating temperature, the particle mass emission indices obtained under the cold condition were plotted against the emission indices obtained under the warm operating condition measured by the nano-SMPS (Fig. 3a). Recall that the "cold" condition refers to a stepwise increase in power during the first part of the engine operating cycle, whereas "warm" is a stepwise decrease in power at the end of the cycle. As shown in Fig. 3a, the data obtained under the warm engine condition were highly linearly correlated (correlation coefficient or $r^2 = 0.94$) with that obtained for cold condition. The slope of 0.92 indicates that the engine had higher efficiency and produced ~8% less PM mass at the warm condition than at the cold condition. This trend is also consistent with data collected by Lobo

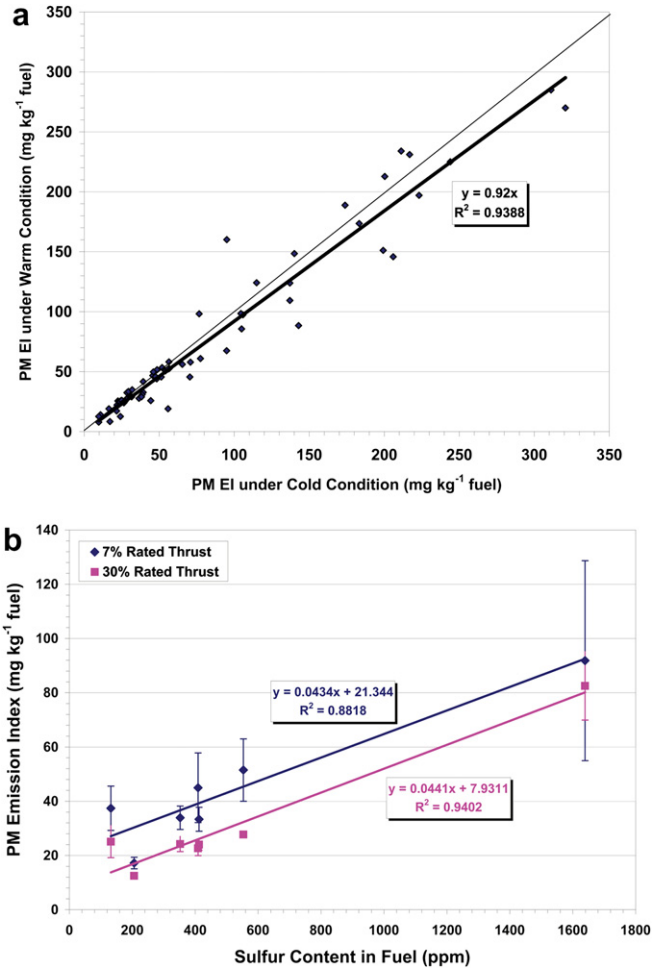

Fig. 3. Effect of: (a) operating temperature; and (b) fuel sulfur on PM mass EI. Fuel sulfur data are for all CFM56 models as determined by the nano-SMPS for 7 and 30% rated thrust. Data points are average values obtained at the same fuel sulfur. T1 of APEX-3 was eliminated from (b) due to cross winds.

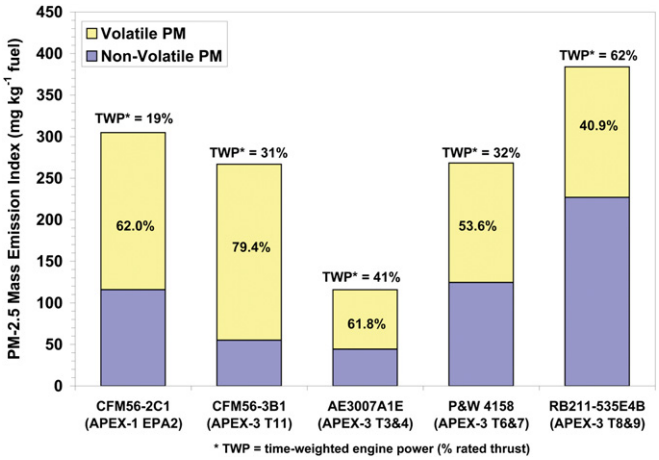

Fig. 4. PM mass emission index and percent volatile fraction as determined by the time-integrated Teflon filter sampling with and without a thermal denuder. Note the difference in time-weighted engine power represented by these samples.

et al. (2007a), and was also observed in terms of particle number as discussed below.

Fuel composition also has a measurable impact on the mass of PM emitted as illustrated in Fig. 3b where the nano-SMPS EI_m is plotted against fuel sulfur for all four CFM56 models tested. Although the nano-SMPS data were only adequate to evaluate the emissions at 7 and 30% engine thrust, all of the data show linear relationships between EI_m and fuel sulfur. Like the particle number emissions discussed below, the high particle mass emissions from the high-sulfur fuel are believed attributable to the formation of additional sulfate particles.

5.2. PM mass emission indices by Teflon filter sampling

The test-average mass emission index obtained by Teflon filter sampling for the CFM56-2C1 engine operating under the EPA cycle and base fuel is compared to similar indices for other engines operating at a variety of time-weighted power (TWP) conditions and with different fuels in Fig. 4. Note that no Teflon filter data are available for APEX-2 due to problems with the gravimetric analyses. Fig. 4 shows that the large, internally mixed flow RB211-535E4-B engine produced the most mass of particles per kg of fuel but had the smallest percentage of volatiles, while the smallest engine, the AE3007A1E (also internally mixed), had the lowest PM mass emission index but produced proportionally more volatiles. In addition, for a range of TWP of 19–62%, the PM emitted from all engines contained ~40–80% volatile matter on a test-average basis with the CFM56 engines generally emitting proportionally more volatile PM (62–80%) as compared to the others tested.

Finally, it must be noted that generally poor agreement was obtained when comparing the nano-SMPS data to that determined by the Teflon filters. When the time-integrated EI_m developed from the Teflon filter sampling were compared to those calculated from the nano-SMPS particle counts, it was found that the Teflon filter samples produced, on average, 118% (relative percent difference) higher EI values and that there was no linear correlation between the two data sets. This is probably at least partially due to a slow instrument response time for the nano-SMPS, which caused gaps in collecting sufficient data points for high thrust runs and transition from one thrust level to another in very short periods of time. Regardless of the cause, the large difference in EI_m obtained by the Teflon filter sampling as compared to SMPS measurements certainly warrants further investigation.

5.3. Particle number emission indices

The particle number emission indices from the nine engine models tested ranged from about 10^{15} to 10^{17} particles kg^{-1} and was found to strongly correlate with fuel flow rate. As was the case for the EI_m, the EI_n vs. fuel flow relationship was similar for all of the turbofan engines tested as can be observed from the EEPS data presented in Fig. 5. As shown in this figure for most of the turbofan engines tested, a logarithmic decline of EI_n with increasing fuel flow (engine power) was determined in the general form:

$$EI_n = m \cdot \ln(\text{fuel flow}) + b \quad (1)$$

where: m = slope of the regression line = $-2(10)^{15}$ to $-3(10)^{16}$; b = intercept of the regression line = $2(10)^{16}$ to $2(10)^{17}$.

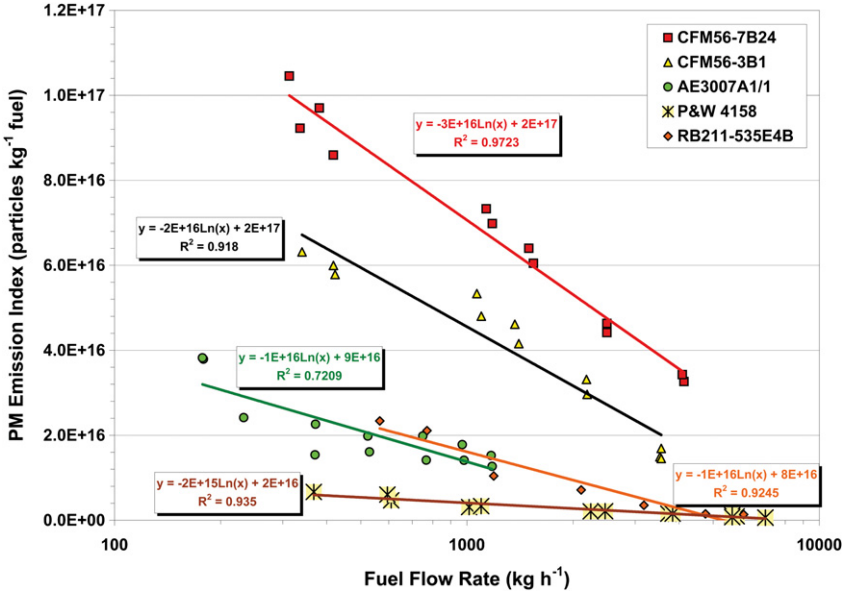

Fig. 5. PM number emission index as a function of fuel flow rate for different engines as determined by the EEPS. Also note logarithmic correlations.

The fuel flow in Equation (1) is expressed in terms of kg h^{-1} and the EI as particles kg^{-1} of fuel burned. The effects of operating temperature and fuel composition on EI_n were found to be similar to those observed for EI_m. With respect to operating temperature, the linear regression results of the "cold" vs. "warm" EI_n data obtained in the three APEX campaigns again showed approximately 8% lower EIs with warm engines which is the same as the EI_m discussed above.

Like the EI_m, the nano-SMPS results again show that the high-sulfur fuel tested in APEX-1 produced higher particle counts at all tested fuel flow rates which is consistent with similar data reported by Wey et al. (2006). When all the CFM56 APEX data were combined, the EI_n generally increased with fuel sulfur except for the very low sulfur (132 ppm) fuel tested in Test 1 of APEX-2. However, the relationship of EI_n to fuel sulfur was more of an exponential function as compared to EI_m which was linear. The higher particle number emissions from the high-sulfur fuel are believed attributable to a small portion of the sulfur in jet fuel being converted into sulfuric acid which could either form nucleates or condense onto the existing aerosol surfaces as the plume cooled (Petzold and Schroder, 1998).

5.4. Particle size distribution

In general, an unimodal and lognormally distributed PSD was observed for most engines and fuel flows except at higher engine power levels where an accumulation mode was found. The magnitude of the accumulation mode varied by engine type as illustrated in Fig. S-3 of the Supporting information for two CFM56 models. The size of the PM emissions also generally ranged from ~3 to 100 nm in electrical mobility diameter.

Probably the best way to compare the PSDs for the various engines tested is to look at the GMD and GSD as a function of fuel flow as shown in Fig. 6. As can be seen in Fig. 6a, all the engines had a GMD of about 10–20 nm at low fuel flow rates, which first decreased and then increased as the fuel flow rate increased. It also appears that, for most of these engines, the GMD was smallest at the fuel flow rate ranging below ~2000 kg h^{-1}. Also, for the two

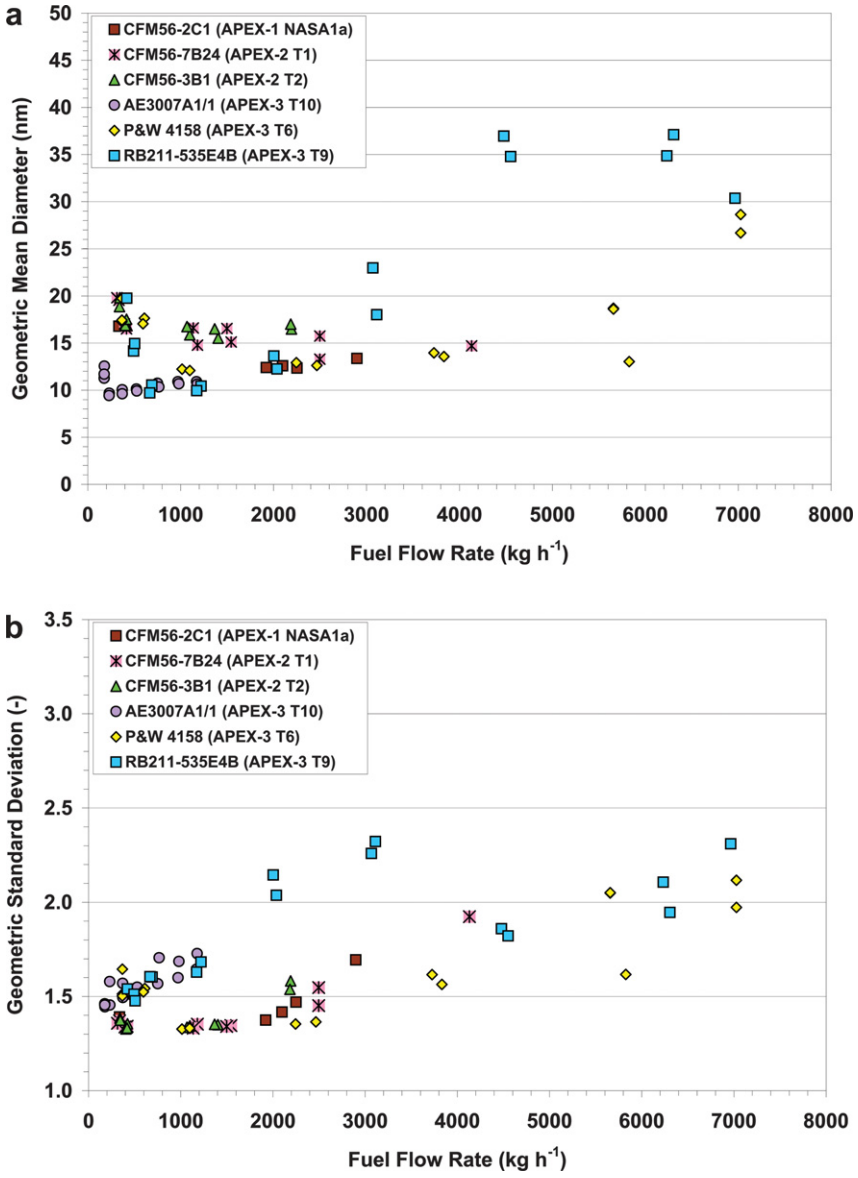

Fig. 6. Comparison of the: (a) geometric number mean particle diameter; and (b) geometric standard deviation vs. fuel flow for different engine types as a function of fuel flow rate.

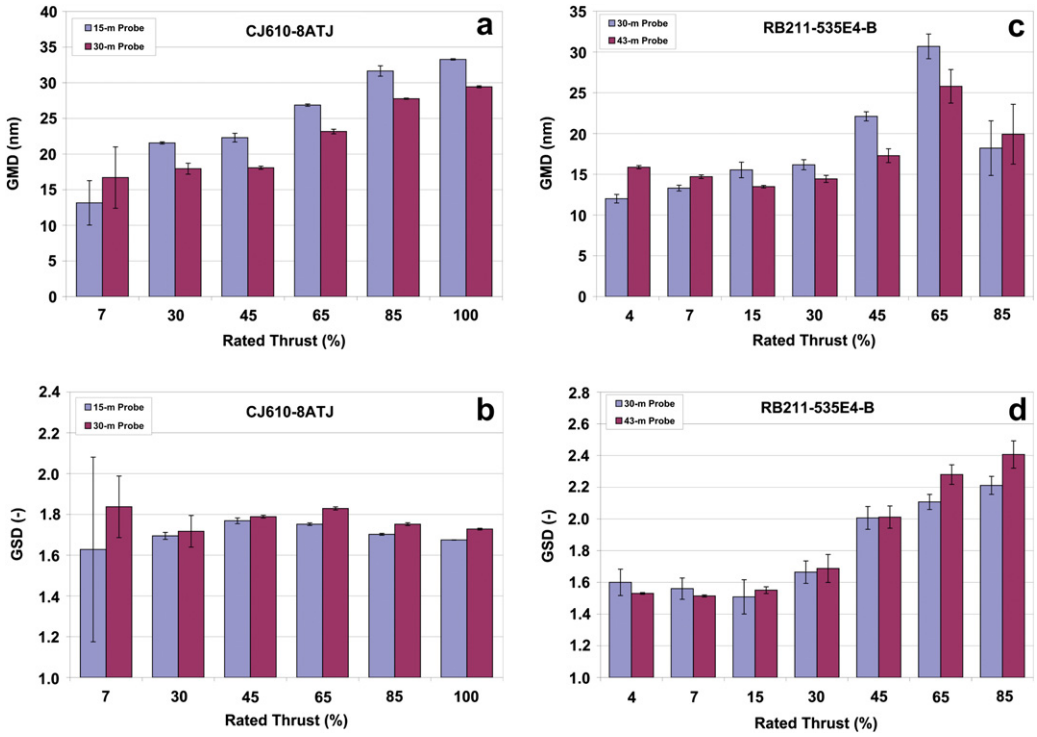

Fig. 7. The effect of plume aging on the GMD (a and c) and GSD (b and d) for two different engines tested in APEX-3. The data were obtained from the nano-SMPS for the CJ610-8ATJ, and the EEPS instrument for the RB211-535E4-B.

largest engines tested, the GMD of the RB211-535E4-B engine increased more sharply in comparison to the P&W 4158 engine as the fuel flow rate increased beyond ~3000 kg h^{-1}.

The GSD results in Fig. 6b show a similar trend in that the GSD first decreased and then increased with increasing fuel flow with the possible exception of the two internally mixed engines (AE3007 and RB211). The overall rise in GMD and GSD when the engines were operated under the higher power settings (higher fuel flow rate) suggest that more accumulation mode particles were formed in the PM emissions thus increasing the overall particle size and broadening the PSD. Similar observations were also made by Lobo et al. (2007a, 2007b) for APEX-1 and -2. Fig. 6 also indicates that the P&W 4158 and RB211-535E4-B engines, which were the largest tested in the APEX campaigns, also had larger GMD and GSD at higher fuel flow rates.

Finally, the effect of sampling probe location (i.e., plume aging) on the PM emissions was investigated in Tests 5 and 8 of APEX-3 as shown in Fig. 7. In these tests, the data were first collected at the probe closest to the engine and increased stepwise in power and then sampled at the farthest probe with the power similarly decreased. As can be seen in Fig. 7a and c for the two engines, the GMDs measured by the probe farthest from the engine were generally lower than that measured by the closest probe except at 7% idle for the CJ610-8ATJ and <15% and 85% thrust for the RB211-535E4-B. As also can be observed from the data in Fig. 7b and d, the aerosol at the farthest probe exhibited a larger GSD than at the probe closest to the engine at all power conditions for the CJ610-8ATJ and >15% rated thrust for the RB211. These results would indicate that at higher engine powers more fine particles were formed in the plume by nucleation and condensation of volatiles as the plume diluted and aged which reduced the average particle size and widened the PSD. At low engine power, however, the opposite trend was seen probably due to the incorporation of volatile organics which are generally higher near idle power.

It should be noted, however, that both new particle nucleation and agglomeration are both taking place as the plume ages as evidenced by the EI_n for the two engines which was always higher at the probe closest to the engine, except at 4 and 7% power for the RB211. The first process is increasing the number of particles whereas the second process is reducing the number of particles. As the accumulation mode forms downstream of the engine, the decrease in particle number may dominate thus reducing the EI_n as observed. Additional research is needed, however, to verify this interpretation of the data.

Appendix. Supporting information

Supporting information associated with this paper can be found, in the online version, at doi:10.1016/j.atmosenv.2010.02.010.

References

Kinsey, J.S., Mitchell, W.A., Squier, W.C., Wong, A., Williams, C.D., Logan, R., Kariher, P.H., 2006. Development of a new mobile laboratory for characterization of the fine particulate emissions from heavy-duty diesel trucks. Journal of Automobile Engineering 220 (D3), 335–345.

Kinsey, J.S., October 2009. Characterization of Emissions from Commercial Aircraft Engines During the Aircraft Particle Emissions Experiment (APEX) 1 to 3. EPA-600/R-091/130. U.S. Environmental Protection Agency, Research Triangle Park, NC.

Lobo, P., Whitefield, P.D., Hagen, D.E., Herndon, S.C., Jayne, J.T., Wood, E.C., Knighton, W.B., Northway, M.J., Miake-Lye, R.C., Cocker, D., Sawant, A., Agrawal, H., Miller, J.W., October 31 2007a. The Development of Exhaust Speciation Profiles for Commercial Jet Engines. Final Report, Contract No. 04-344. California Air Resources Board, Sacramento, CA. Available at: http://www.arb.ca.gov/research/apr/past/mobile.htm.

Lobo, P., Hagen, D.E., Whitefield, P.D., Alofs, D.J., 2007b. Physical characterization of aerosol emissions from a commercial gas turbine engine. Journal of Propulsion and Power 23, 919–929.

Penner, J.E., Lister, D.H., Griggs, D.J., Dokken, D.J., McFarland, M., 1999. Aviation and the Global Atmosphere. Cambridge University Press.

Petzold, A., Schroder, F.P., 1998. Jet engine exhaust aerosol characterization. Aerosol Science & Technology 28, 62–76.

Sausen, R., Isaksen, I., Grewe, V., Hauglustaine, D., Lee, D.S., Myhre, G., Kohler, M.O., Pitari, G., Schumann, U., Stordal, F., Zerefos, C., 2005. Aviation radiative forcing in 2000: an update on IPCC 1999. Meteorologische Zeitschrift 14, 555–561.

Waitz, I.A., Townsend, J., Cutcher-Gershenfeld, J., Greitzer, E., Kerrebrock, J., December 2004. Aviation and the Environment. Report to the United States Congress, Partnership for AiR Transportation Noise and Emissions Reduction. Massachusetts Institute of Technology, Cambridge, MA.

Wayson, R.L., Fleming, G.G., Iovinelli, R., 2009. Methodology to estimate particulate matter emissions from certified commercial aircraft engines. Journal of the Air & Waste Management Association 59, 91–100.

Webb, S., Whitefield, P.D., Miake-Lye, R.C., Timko, M.T., Thrasher, T.G., 2008. Research Needs Associated with Particulate Emissions at Airports. ACRP Report 6. U.S. Transportation Research Board of the National Academies, Washington, D. C.

Wey, C.C., Anderson, B.E., Hudgins, C., Wey, C., Li-Jones, X., Winstead, E., Thornhill, L. K., Lobo, P., Hagen, D., Whitefield, P., Yelvington, P.E., Herndon, S.C., Onasch, T.B., Miake-Lye, R.C., Wormhoudt, J., Knighton, W.B., Howard, R., Bryant, D., Corporan, E., Moses, C., Holve, D., Dodds, W., 2006. Aircraft Particle Emissions Experiment (APEX). NASA/TM-2006-214382, ARL-TR-3903. U.S. National Aeronautics and Space Administration, Glenn Research Center, Cleveland, OH. Available at: http://gltrs.grc.nasa.gov.

Wey, C.C., Anderson, B.E., Wey, C., Miake-Lye, R.C., Whitefield, P., Howard, R., 2007. Overview of the aircraft particle emissions experiment. Journal of Propulsion and Power 23, 898–905.

Wuebbles, D., Gupta, M., Ko, M., 2007. Evaluating the impacts of aviation on climate change. EOS Transactions American Geophysical Union 88, 157–168.